



Quantitative determination of the structures of Bi and Sb thin films grown on Si(111) and Ge(111) surfaces
by Kejia Wan

A thesis submitted in partial fulfillment of the requirements for the degree of Doctor of Philosophy in Physics
Montana State University
© Copyright by Kejia Wan (1991)

Abstract:

ABSTRACT The modification of metal-semiconductor interface structures is a very interesting topic, and the geometric structure of such surfaces is a central issue in semiconductor physics. An entire experimental system containing low energy electron diffraction, Auger electron spectroscopy and thin film sample preparation and characterization apparatus has been developed. The computer program for the theoretical analysis of LEED I-V curves has been established. The surface reconstructions of semiconductor Si(111) and Ge(111) due to the adsorption of column-V metal atoms such as Bi and Sb have been studied by this technique. The initial epitaxial growth process and the ordering phenomena were studied as a function of overlayer coverage and deposition conditions.

For the Bi/Si(111) system, our experiments show that two equilibrium phases are formed in the growth process, each displaying a $(\sqrt{3}\times\sqrt{3})$ -R30° LEED symmetry: an α -phase occurring at 1/3 ML Bi coverage and substrate temperature of 360° C, and a β -phase at 1 ML and 300° C. For the Bi/Ge(111) system, only one $(\sqrt{3}\times\sqrt{3})$ phase was obtained at the 1/3 ML coverage and 380° C substrate temperature. For Sb overlayers, the Si(111) surface exhibits a series of phases with the $(\sqrt{3}\times\sqrt{3})$ structure being the most stable, which appears at 1 ML coverage and 550° C substrate temperature. In contrast, for the Ge(111) substrate, only the ordered (1x1) structure was observed at an Sb coverage of 1 ML and thermal annealing to 380° C.

Quantitative structural information for each system was determined by multiple scattering analysis of I-V curves. The analysis is facilitated by comparing LEED intensity data measured for each phase with calculated values using appropriate structural models.

For the $(\sqrt{3}\times\sqrt{3})$ surfaces, the T4 geometry for the 1/3 ML case and a timber geometry for the 1 ML case are found to be the best models, while substitution model is responsible for the 1 ML (1x1) surface. The detailed atomic coordinates have been determined for each system.

The surface reconstructions of the above (111) surfaces are discussed in terms of the atomic size effect and chemical bonding nature of the adsorbate and substrate. An understanding of the atomic geometry of the epitaxial overlayers is needed to describe more fully the adatom-induced surface reconstruction. The results could in principle be useful in understanding the origin of the adatom-induced surface reconstruction, and could be important in conjunction with structural studies based on calculations of the total energy versus distortion parameters. The method established from this thesis can eventually be applied to study MBE samples.

QUANTITATIVE DETERMINATION OF THE
STRUCTURES OF Bi AND Sb THIN FILMS GROWN
ON Si(111) AND Ge(111) SURFACES

by
Kejia Wan

A thesis submitted in partial fulfillment
of the requirements for the degree

of

Doctor of Philosophy

in

Physics

MONTANA STATE UNIVERSITY
Bozeman, Montana

July, 1991

APPROVAL

of a thesis submitted by

Kejia Wan

This thesis has been read by each member of the thesis committee and has been found to be satisfactory regarding content, English usage, format, citations, bibliographic style, and consistency, and is ready for submission to the College of Graduate Studies.

July 15, 1991
Date


Chairperson, Graduate Committee

Approved for the Major Department

July 15, 1991
Date


Head, Major Department

Approved for the College of Graduate Studies

July 19, 1991
Date


Graduate Dean

STATEMENT OF PERMISSION TO USE

In presenting this thesis in partial fulfillment of the requirements for a doctoral degree at Montana State University, I agree that the Library shall make it available to borrowers under rules of the Library. I further agree that copying of this thesis is allowable only for scholarly purposes, consistent with "fair use" as prescribed in the U. S. Copyright law. Requests for extensive copying or reproduction of this thesis should be referred to University Microfilms International, 300 North Zeeb Road, Ann Arbor, Michigan 48106, to whom I have granted "the exclusive right to reproduce and distribute copies of the dissertation in and from microfilm and the right to reproduce and distribute by abstract in any format."

Signature Kejia Wan

Date July 7, 1991

ACKNOWLEDGMENTS

The author owes a special debt of gratitude to some individuals who provided thoughtful advice and encouragement in carrying out the work performed for this thesis. Foremost, the author wishes to thank his two advisors, Dr. W. K. Ford, for his guidance and unlimited advice during all stages of this work; Dr. J. C. Hermanson, for his stimulating discussion, his kindness, and his critical reading of my scientific papers including this thesis.

The author also acknowledges Dr. T. Guo for his important guidance, helpful discussion, and technical assistance. Special thanks go to G. J. Lapeyre, J. Anderson, R. J. Smith, J. Carlsten, A. Eguluz, and R. T. Robiscoe for their support and advice.

Thanks are due to the staff and fellow graduate students in the Physics Department, M. S. U.

Finally, he wishes to dedicate all his accomplishments to his wife and parents for their spiritual encouragement and support over a number of years.

TABLE OF CONTENTS

	Page
ACKNOWLEDGEMENTS	iv
LIST OF TABLES	vii
LIST OF FIGURES	viii
ABSTRACT	xi
1. INTRODUCTION.....	1
2. EXPERIMENTAL METHOD AND TECHNIQUES	6
Surface Crystallography and Low Energy Electron Diffraction	6
Surface Classification.....	6
Low Energy Electron Diffraction (LEED).....	11
Auger Electron Spectroscopy	17
Experimental Apparatus	19
Experimental Layout	21
LEED Mode.....	21
Auger Mode.....	22
Data Acquisition	23
Software.....	24
Sample preparation.....	24
Sample Cleaning.....	24
Thin Films Deposition.....	27
QCO Calibration.....	27
3. MULTIPLE SCATTERING THEORY.....	29
Introduction.....	29
Kinematic Theory to Dynamical Theory.....	29
The Intensity Calculation in Dynamical Theory.....	31
Ion-core Scattering	32
Phase Shifts.....	33
Inelastic Effects.....	35
Thermal Vibration	38
Multiple Scattering	38
Duke and Laramore Method.....	43
From Theory to Computer Program	44
4. COMPUTER PROGRAM.....	46
Description of Code.....	46
Phase Shifts Calculation.....	48
Intensity Calculation: Main Program.....	49

TABLE OF CONTENTS - Continued

	Page
Data Evaluation	51
Simplex Algorithm.....	53
The Code Testing.....	54
5. GEOMETRIC STRUCTURES OF THIN BISMUTH AND ANTIMONY FILMS ON Si(111) SUBSTRATES	56
Introduction	56
Experimental Details	57
Measurements.....	57
Beam Index Convention.....	58
Incident Electron Beam Alignment.....	60
The Bi/Si(111) System	62
Experimental Results.....	62
Discussion of Data	70
Dynamical Calculation.....	72
Growth Discussion.....	88
The Sb/Si(111) System.....	89
Experimental Results.....	89
Discussion.....	91
6. GEOMETRIC STRUCTURES OF THIN BISMUTH AND ANTIMONY FILMS ON Ge(111) SUBSTRATES	95
Introduction	95
Experimental Details	96
The Bi/Ge(111) System.....	96
Experimental Results.....	96
Dynamical LEED Calculation.....	101
Discussion.....	105
Summary	106
The Sb/Ge(111) System.....	106
Experimental Observation	106
Dynamical Calculation.....	109
7. DISCUSSION OF COLUMN-V ADSORBATES ON Si(111) AND Ge(111); SUMMARY	115
Bonding Behavior.....	115
Summary	120
REFERENCES CITED.....	122

LIST OF TABLES

Table	Page
1 QCO frequencies for 1 ML adsorbates on Si(111) and Ge(111) substrates	28
2 A succession of scattering for two atoms.....	40
3 Results of the dynamical LEED analysis for the α -phase and β -phase. The structural models are the trimer model for the β -phase and the T ₄ model for the α -phase. cf. Fig.26. and 27	80
4 Atomic coordinates of the α -phase structure; cf. Fig. 26	83
5 Atomic coordinates of the β -phase structure; cf. Fig. 27	84
6 Atomic coordinates of the T ₄ structure: the Cartesian coordinates and atom numbers are defined according to Fig.26 (b) of chapter 5. The origin is placed at the topmost Bi atom.....	103
7 Surface atom deformation induced by the Bi adatom. cf. Fig. 26 (b).....	105
8 Summary of ordering structures of column-V elements over Si, Ge(111) surfaces..	115
9 Comparison of substrate deformation for optimal T ₄ structures. The parameters are defined according to Fig. 26	119

LIST OF FIGURES

Figure	Page
1 The five types of two-dimensional Bravais lattices.....	8
2 The $(\sqrt{3}\times\sqrt{3})$ structure in reciprocal space and possible atomic arrangement in real space.....	10
3 The principle of the formation of a diffraction pattern in LEED experiment.....	13
4 Some examples of surface defects, the corresponding modification of the reciprocal lattice rods and the resultant LEED spot profile.....	16
5 Schematic of Auger process.....	18
6 Schematic diagram of the LEED experimental system.....	20
7 Circuit for using LEED system as a retarding field analyzer.....	22
8 The sample holder for Si wafer sample.....	25
9 The Ge sample for cleaving and the sample holder.....	26
10 Schematic description of the individual atom and point scattering.....	32
11 "Universal Curve" of electron mean free path as a function of electron kinetic energy.....	37
12 Multiple scattering of a spherical wave by two atoms, showing Green's function notation.....	40
13 Generalized flowchart of dynamical LEED program.....	47
14 I-V curves of the known Si(111)- $\sqrt{3}\times\sqrt{3}$ - Ga structure calculated by current program. c.f. Ref.[10].....	55
15 The LEED image of Si(111)- 7×7 clean surface,taken at 35.6 eV.....	59
16 The LEED image of Si(111)- $\sqrt{3}\times\sqrt{3}$ -Bi surface, taken at 45.1 eV.....	59
17 Beam notations in k-space for the Si(111)- $\sqrt{3}\times\sqrt{3}$ -Bi surface. k-k', h-h', and j-j' are symmetry axes.....	60
18 Illustration of symmetry relationships for six lowest integral-order beams.....	61
19 Dependence of (1,0) beam intensity on Bi coverage for Bi/Si(111).....	63

LIST OF FIGURES - Continued

20	The I-V curves for the β -phase	66
21	The I-V curves for the α -phase	67
22	(a) (1 0) and (b) (1/3 1/3) beams I-V curves; comparison of different sample preparations.....	68
23	Bi (96 and 101 eV) Auger line intensity vs annealing temperature for 1.5 ML coverage on a Si(111) surface.....	70
24	Energy-dependent phase shifts used in the theoretical calculations: (a) Bi; (b) Sb; (c) Si; (d) Ge. The relativistic Hartree-Fock-Slater crystal potential model with Hara exchange was used.....	74
25	Total elastic cross sections of Bi, Sb adatoms and Si, Ge substrate atoms from the phase shifts shown in Fig. 24 and plotted as a function of incident beam energy ...	75
26	(a) Top and (b) side views of the optimized structure for α -phase: T ₄ model.....	77
27	(a) Top and (b) side views of the optimized structure for β -phase: trimer model....	78
28	Comparison between experimental and calculated IV spectra for the α -phase; the solid curves are taken from experimental data and dashed lines show the computed intensities of the best fit structural model in Fig. 26. (a) integral spots. (b) fractional spots. Averaged R _x is 0.233. Eleven LEED beams were included in the analysis.	81
29	Comparison between experimental and calculated IV spectra for the β -phase; the solid curves are taken from experimental data and dashed lines show the computed intensities of the best fit structural model in Fig. 27. (a) integral spots. (b) fractional spots. Averaged R _x is 0.225	82
30	Variation of R _x with some parameters described in Fig. 24 for the α -phase structure. The other model parameters used are those listed in Table 2	86
31	Variation of R _x with some parameters described in Fig. 27 for the β -phase structure. The other model parameters used are those listed in Table 2	87
32	Sb/Si(111) phase diagram	91
33	The I-V curves for Si(111)- $\sqrt{3}\times\sqrt{3}$ -Sb surface.....	92
34	Dependence of (1,0) beam intensity on Bi coverage for Bi/Ge(111).....	98

LIST OF FIGURES - Continued

35	Bi (96 and 101 eV) Auger line intensity vs annealing temperature for 1.5 ML coverage on Ge(111) surface. The range of observed LEED symmetry is also indicated.....	99
36	I-V spectra for two different sample preparations to demonstrate the similarity of the LEED structures. The solid lines refer to hot substrate deposition at 320°C and the dashed lines refer to room temperature substrate deposition followed by annealing. The relative intensities of the beams are retained within each panel. (a) integral-order spots; (b) fractional-order spots.....	100
37	Comparison between experimental and calculated I-V spectra; solid curves are from experimental data and dashed lines are the computed intensities of the best-fit structural model. (a) integral-order spots; (b) fractional-order spots. Averaged R_x (eleven beams) is 0.244.....	102
38	Variation of R_x with the substrate deformation parameter (a) and vertical height of Bi atom (b) for the best fit structure to demonstrate the occurrence of local minima.....	104
39	(1,0) beam dependence on Sb coverage for Sb/Ge(111) system	108
40	I-V curves of Sb/Ge(111) 1×1 surface; five low index beams are presented.....	109
41	The model for Sb/Ge(111) 1×1 surface.....	111
42	Variation of R_x as a function of d_{12}	113
43	Comparison between experimental and calculated I-V curves for the two models.....	114
44	Adatom structure for T ₄ models	119

ABSTRACT

The modification of metal-semiconductor interface structures is a very interesting topic, and the geometric structure of such surfaces is a central issue in semiconductor physics. An entire experimental system containing low energy electron diffraction, Auger electron spectroscopy and thin film sample preparation and characterization apparatus has been developed. The computer program for the theoretical analysis of LEED I-V curves has been established. The surface reconstructions of semiconductor Si(111) and Ge(111) due to the adsorption of column-V metal atoms such as Bi and Sb have been studied by this technique. The initial epitaxial growth process and the ordering phenomena were studied as a function of overlayer coverage and deposition conditions.

For the Bi/Si(111) system, our experiments show that two equilibrium phases are formed in the growth process, each displaying a $(\sqrt{3}\times\sqrt{3})$ -R30° LEED symmetry: an α -phase occurring at 1/3 ML Bi coverage and substrate temperature of 360° C, and a β -phase at 1 ML and 300 °C. For the Bi/Ge(111) system, only one $(\sqrt{3}\times\sqrt{3})$ phase was obtained at the 1/3 ML coverage and 380 °C substrate temperature. For Sb overlayers, the Si(111) surface exhibits a series of phases with the $(\sqrt{3}\times\sqrt{3})$ structure being the most stable, which appears at 1 ML coverage and 550 °C substrate temperature. In contrast, for the Ge(111) substrate, only the ordered (1×1) structure was observed at an Sb coverage of 1 ML and thermal annealing to 380 °C.

Quantitative structural information for each system was determined by multiple scattering analysis of I-V curves. The analysis is facilitated by comparing LEED intensity data measured for each phase with calculated values using appropriate structural models. For the $(\sqrt{3}\times\sqrt{3})$ surfaces, the T₄ geometry for the 1/3 ML case and a trimer geometry for the 1 ML case are found to be the best models, while substitution model is responsible for the 1 ML (1×1) surface. The detailed atomic coordinates have been determined for each system.

The surface reconstructions of the above (111) surfaces are discussed in terms of the atomic size effect and chemical bonding nature of the adsorbate and substrate. An understanding of the atomic geometry of the epitaxial overlayers is needed to describe more fully the adatom-induced surface reconstruction. The results could in principle be useful in understanding the origin of the adatom-induced surface reconstruction, and could be important in conjunction with structural studies based on calculations of the total energy versus distortion parameters. The method established from this thesis can eventually be applied to study MBE samples.

CHAPTER 1

INTRODUCTION

Semiconductor physics is closely related to the development of semiconductor technology. The demand to improve device performance requires the understanding of physical processes in semiconductor material. On the other hand, the rapid development in modern technology has made it possible to produce higher-quality semiconductor devices. Since devices have reached a high level of integration such that surface and interface effects play an important role in determining the characteristics of performance, the study of semiconductor surfaces is one of the major efforts in surface science.¹

During the past decade, nonequilibrium techniques have been developed for the study of electronic and geometric properties of semiconductor surfaces. Electronic properties near the surface and interface region, such as Schottky barrier formation and Fermi level pinning, are of great practical interest in the manufacture of microelectronics devices. However, a more fundamental, or more microscopic, understanding of these properties depends on knowing the atomic structure of such surfaces. The change in atomic geometry at a surface or interface relative to the bulk involves a variety of factors, including changes in surface work function, the introduction of surface electronic states, vibrational modes, surface strain fields, and a wide range of chemisorption and heterogeneous catalytic phenomena. Therefore, the description of surface electronic properties is greatly improved if the surface atomic structure is known.

Geometric structures with atomic dimensions give rise to new phenomena resulting from quantum-mechanical effects, e.g., low-energy electron diffraction (LEED).² Layered structures with a periodicity of a few atomic layers result in coherent behavior for long-range bonding such as ordered interfaces in metal-semiconductor systems. Studies of the geometric structure of metal-semiconductor interfaces have led to significant advances in our basic understanding of the physics of materials as well as to important new technologies. Two aspects of surface structural determination have been investigated extensively by both experiment and theory: the atomic geometries of semiconductor surfaces and interfaces, and the character of the chemical bond between atomic species at surfaces and interfaces. These two issues are emphasized in this thesis. To date, silicon is the most common material in semiconductor technology, and along with germanium and GaAs, is one of the three most important semiconductors.³

Much effort has been devoted to the study of the morphology and growth characteristics of metal films on Si, Ge and GaAs, especially films of column-III and column-V elements on Si and Ge. Bismuth and antimony exhibit some interesting properties in connection with metallization in Si device technology.⁴ In the studies of metal-III-V semiconductor contacts, bismuth and antimony are found to be among the very few metals that form ordered monolayers on III-V(110) semiconductor surfaces.⁵ They exhibit adsorption size effects, indicating that two-dimensional island formation below 1 ML, and interesting surface bonding properties.⁶ Thus, both bismuth and antimony adsorption have attracted great interest. In this thesis, we use low-energy electron diffraction (LEED) and Auger spectroscopy (AES) to study Bi and Sb epitaxy on Si(111) and Ge(111) surfaces. This study serves to characterize the types of overlayer formation that occur for column-V atoms on Si and Ge substrates.^{7,8} One main thrust of this thesis is to categorize the growth and ordering characteristics according to the atomic size of adatom

and substrate and the chemical nature of their bonding, and to emphasize the differences we observe in the epitaxial behavior of these elements.

When metal atoms (or molecules) are adsorbed onto a semiconductor surface, the adsorbates can be trapped in a potential energy well on the surface. If the surface exhibits long-range two-dimensional periodicity, ordered adlayers can result from the interactions between adsorbate atoms and from the site-dependent interactions between adparticles and substrate. Extensive adsorption studies have been carried out on Si(111) and Ge(111) substrates for the past decade. The adsorption of metal overlayers in the submonolayer range on Si or Ge(111) surfaces can result in surface superstructures with a variety of phases. Among those phases, the ordered $(\sqrt{3}\times\sqrt{3})R30^\circ$ reconstruction is the most frequently observed structure. This reconstruction often appears when column III (Al, Ga, In)⁹⁻¹¹, column IV (Sn,Pb)^{12,13}, or column V (Sb, Bi)^{14,15} atoms are adsorbed on clean Si(111) or Ge(111) surfaces. Some other metals such as Ag and Au also induce this reconstruction. The coverage of the metal films may be 1/3 to 4/3 monolayers depending on the individual group. Models of the $(\sqrt{3}\times\sqrt{3})$ reconstruction have been proposed on the basis of surface total-energy calculations or experimental observations for coverages of 1/3, 2/3, 1, and 4/3 monolayers.^{16-18,13} On the other hand, As induces a (1×1) structure on both Si and Ge(111) surfaces.^{19,20}

The physical origin of adatom-induced surface reconstruction has previously been studied in terms of the surface total energy.^{21,22} An ideal bulk-terminated (111) surface with all atoms located at their ideal bulk positions is not physically realized since it is not at the surface-free-energy minimum, because of the existence of dangling bonds, which are energetically costly. Column-III and column-V adatoms on (111) surfaces saturate the surface dangling bonds, lowering the surface energy. This behavior is described in terms of the chemical bonding between the adsorbate and substrate atoms. Column-III (Al, Ga, In) adatoms induce a $(\sqrt{3}\times\sqrt{3})$ reconstruction on the Si(111) surfaces. The adatom is

believed to be positioned in either the filled site above the second layer Si atoms (T_4) or in the hollow site above the fourth layer Si atoms (H_3), both sites are energetically stable: three substrate dangling bonds can be passivated by one adsorbate atom in an sp^3 bonding geometry.²¹

Column-V As overlayers produce a (1×1) surface unit cell on both Si(111) and Ge(111) surfaces. The As atom has been shown to substitute for the top-most substrate atom to achieve the optimal bonding configuration of both substrate atoms and As atoms: tetrahedral coordination with sp^3 hybridized bonding orbitals for the substrate atoms and p^3 three-fold bonding for the As atoms. Antimony and bismuth adatoms, by contrast, can induce a complex phase diagram including a $(\sqrt{3} \times \sqrt{3})$ structure. The structural phases depend on the adatom coverage and the thermal environment. Recent structural studies have demonstrated that the $(\sqrt{3} \times \sqrt{3})$ surface reconstruction has trimer adatoms in each $(\sqrt{3} \times \sqrt{3})$ site.¹⁸ The center of the trimer could be located at either the T_4 or the H_3 site. To date it has not been possible, however, to obtain conclusive experimental evidence for either geometry, and details of the atomic positions remain unknown.

Among the several techniques for locating atoms at surfaces, low-energy electron diffraction (LEED) is still a powerful tool, though other techniques like photoelectron diffraction and electron holography are advancing rapidly.²³ LEED has been applied successfully to a number of metal and semiconductor surfaces.²⁴ The purpose of this thesis is to accomplish a complete LEED analysis using both experiment and calculation, in order to investigate systematically the structure of the column-V elements adsorbed on Si(111) and Ge(111) substrates. The results could in principle be useful in understanding the origin of the adatom-induced surface reconstructions, and could be important in conjunction with structural studies based on calculations of the total energy versus distortion parameters.

The thesis is organized as follows. Descriptions of surface analysis techniques we used and the experimental set-up, with emphasis on LEED, are given in Chapter 2. The experimental procedures are also discussed there. In Chapter 3, the dynamical LEED theory is reviewed in order to give the basic picture and appropriate physical ingredients for dealing with the calculation of diffraction intensity of the scattered electron beam. The more rigorous general quantum mechanical derivation can be found in the literature. Chapter 4 describes the computational method and computer program used to do LEED intensity analysis; the program is based on the theoretical treatment described in Chapter 3. The studies of Sb, Bi adsorbed on Si(111) and Ge(111) are presented in Chapters 5 and 6, respectively. Chapter 7 presents a comprehensive discussion and summary.

The work in this thesis was initiated by a desire to study the reconstructions of the MBE-grown GaAs surface. The experimental apparatus is compatible with the MBE growth system in the CRISS laboratory in the Physics Department. The computer program can deal with the reconstructions of GaAs(111) surfaces, as well as the (100) surface with some modification. Thus, the method established in this thesis can eventually be applied to study MBE-grown samples.

CHAPTER 2

EXPERIMENTAL METHOD AND TECHNIQUES

In the study of the geometric structure of semiconductor surfaces, it is important to understand the experimental facilities, the analytical techniques, and the procedure used in the experiments. Low energy electron diffraction (LEED) and Auger electron spectroscopy (AES) are used to study metallic thin films grown on Si and Ge surfaces. In this chapter, the experimental techniques, the ultra high vacuum chamber, and the instrumentation used in our work are described.

Surface Crystallography and Low Energy Electron Diffraction

Since a full description of the LEED technique can be found in a number of publications,^{24,25} only some basic concepts and methods related to the thesis work are discussed here.

Surface Classification

The classification and description of the geometric structure of bulk crystalline materials is based on the language of crystallography. Many properties of solids are intimately related to the special symmetry properties of those materials. While a solid surface is intrinsically different from a crystalline solid, in that the three-dimensional periodicity of the structure is reduced to two, the atomic arrangement retains two-

dimensional periodicity parallel to the surface, and this periodicity is an important factor in determining some of the properties of the surface. In particular, periodicity is essential allowing electron diffraction techniques to provide information on the structure of the surface.²⁴ Thus, a proper understanding of surface crystallography is necessary if one wishes to understand the LEED technique.

By surface geometric structure we mean the atomic geometry of the solid in the vicinity of the surface. The surface can be thought of as a substrate which is bulk-like plus the few atomic layers near the surface, which may be deformed relative to bulk layers. For example, it is common that surface relaxation (displacements perpendicular to the surface) and surface reconstruction (displacements parallel to the surface) occur. Surface relaxation and reconstruction involve either the topmost atom strain due to the breaking of three-dimensionality, or involve foreign atom adsorption, called adatoms in both cases. We will use the term overlayer structure to describe those layers of the surface. Evidently, for ordered surfaces, the periodicity of the overlayer structure is frequently in registry with the substrate periodicity, an important factor in our further discussion. The surface symmetry is characterized by its associated unit mesh which must be consistent with one of the 14 Bravais space lattices. Full descriptions of the various Bravais lattices can be found in the literature.²⁵ There are five possible distinct two-dimensional Bravais lattices, which are shown in Fig. 1; \mathbf{a}_1 and \mathbf{a}_2 are primitive translation vectors defining the surface unit mesh, and are generally selected to form the smallest possible parallelogram which preserves the surface symmetries.

In discussing the overlayer structure it is helpful to use a notation which minimizes ambiguities. There are two schemes to relate overlayer structure to that of the underlying substrate. One scheme proposed by Park and Madden (1968) involves a simple vectorial construction,²⁶ which relates the substrate primitive translation vectors ($\mathbf{a}_1, \mathbf{a}_2$) to those of the overlayer ($\mathbf{b}_1, \mathbf{b}_2$) with transformation matrix \mathbf{G} , such that

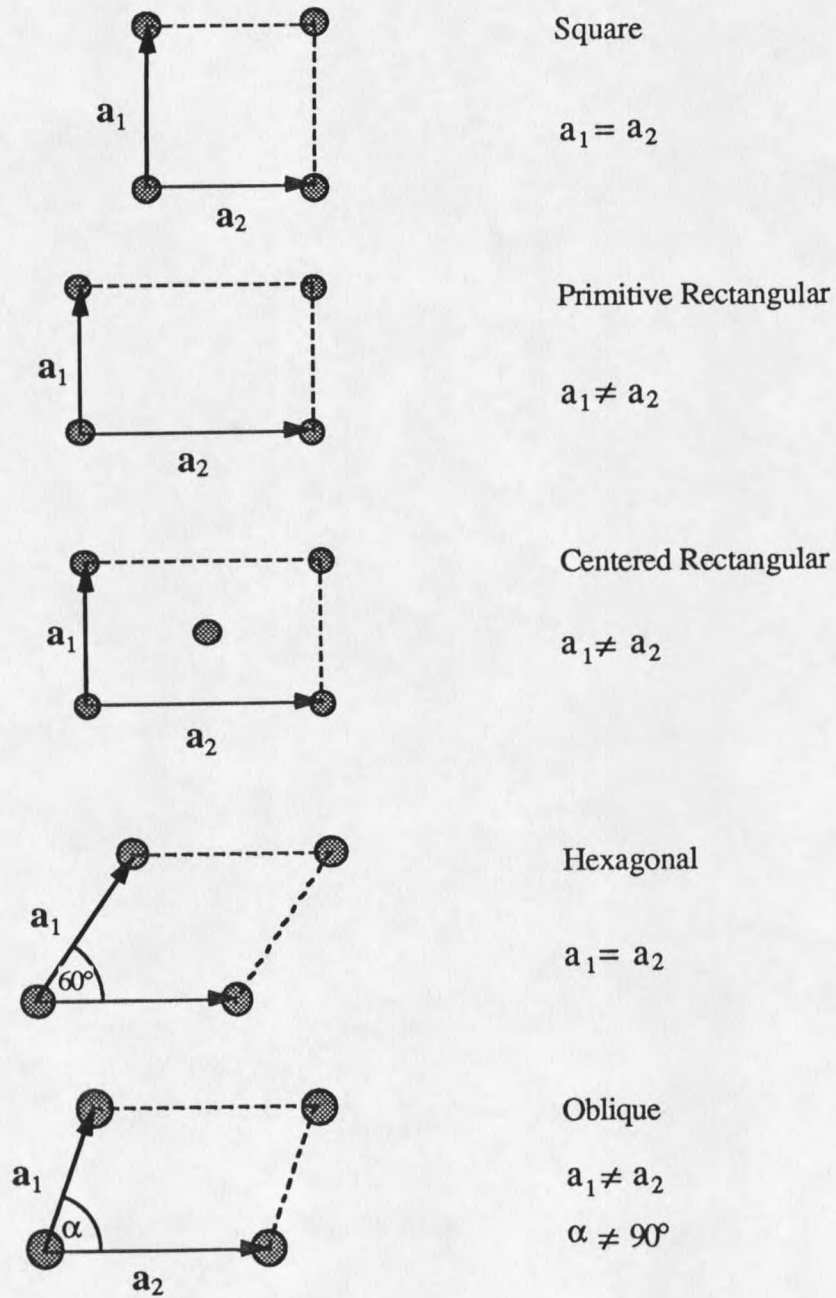


Fig. 1: The five types of two-dimensional Bravais lattices

$$b_1 = G_{11} a_1 + G_{12} a_2$$

$$b_2 = G_{21} a_1 + G_{22} a_2$$

or

$$(b_1, b_2) = G (a_1, a_2) \quad (2.1)$$

The advantage of this notation is that, because the area of the substrate unit mesh is given by $|a_1 \times a_2|$, the determinant of G is simply the ratio of the areas of the two meshes and provides a convenient classification system for the type of overlayer structure. When all components of G are integers, the overlayer structure is called *simple* and the adatom mesh has translation symmetry elements in common with the surface as a whole; if G contains both integers and rational numbers, the overlayer structure is referred to as a *coincidence* structure and the adatom mesh and substrate mesh come into coincidence at regular intervals. When G contains irrational numbers, the overlayer structure is called *incoherent* or *incommensurate*. A disadvantage of this notation is that it doesn't provide an intuitive picture of what the structure looks like.

A more convenient notation for overlayer structure suggested by Wood(1964) is more widely used.²⁷ In this case the notation defines the ratio of the lengths of the surface and substrate meshes, together with the angle through which one mesh must be rotated to align the two pairs of primitive translation vectors. In this notation if adsorbate A on the $\{hkl\}$ surface of material X causes the formation of a structure having primitive translation vectors of length $|b_1| = p|a_1|$ and $|b_2| = q|a_2|$ with a unit mesh rotation of ϕ the structure is referred to as $X \{hkl\} - p \times q - R\phi^\circ - A$. Note that the surface unit mesh is labelled as either centered (c), or primitive (p). In a centered unit mesh a lattice point is found in the center of the surface unit mesh. This method is simple and applicable to a large number of structures, including the III-V(110)-(1 \times 1,1 \times 2,1 \times 3)-(Bi, Sb) system we studied

previously⁶ and the Si, Ge(111)- $\sqrt{3}\times\sqrt{3}$ -(Bi,Sb) systems studied here. Using G matrix notation, the above structures can be expressed as $\begin{pmatrix} 1 & 0 \\ 0 & 1 \end{pmatrix}$, $\begin{pmatrix} 1 & 0 \\ 0 & 2 \end{pmatrix}$, $\begin{pmatrix} 1 & 0 \\ 0 & 3 \end{pmatrix}$, and $\begin{pmatrix} 1/3 & 0 \\ 0 & 1/3 \end{pmatrix}$, respectively. As an example, the atomic arrangement and the LEED pattern of a $(\sqrt{3}\times\sqrt{3})$ structure with this scheme are presented in Fig. 2.

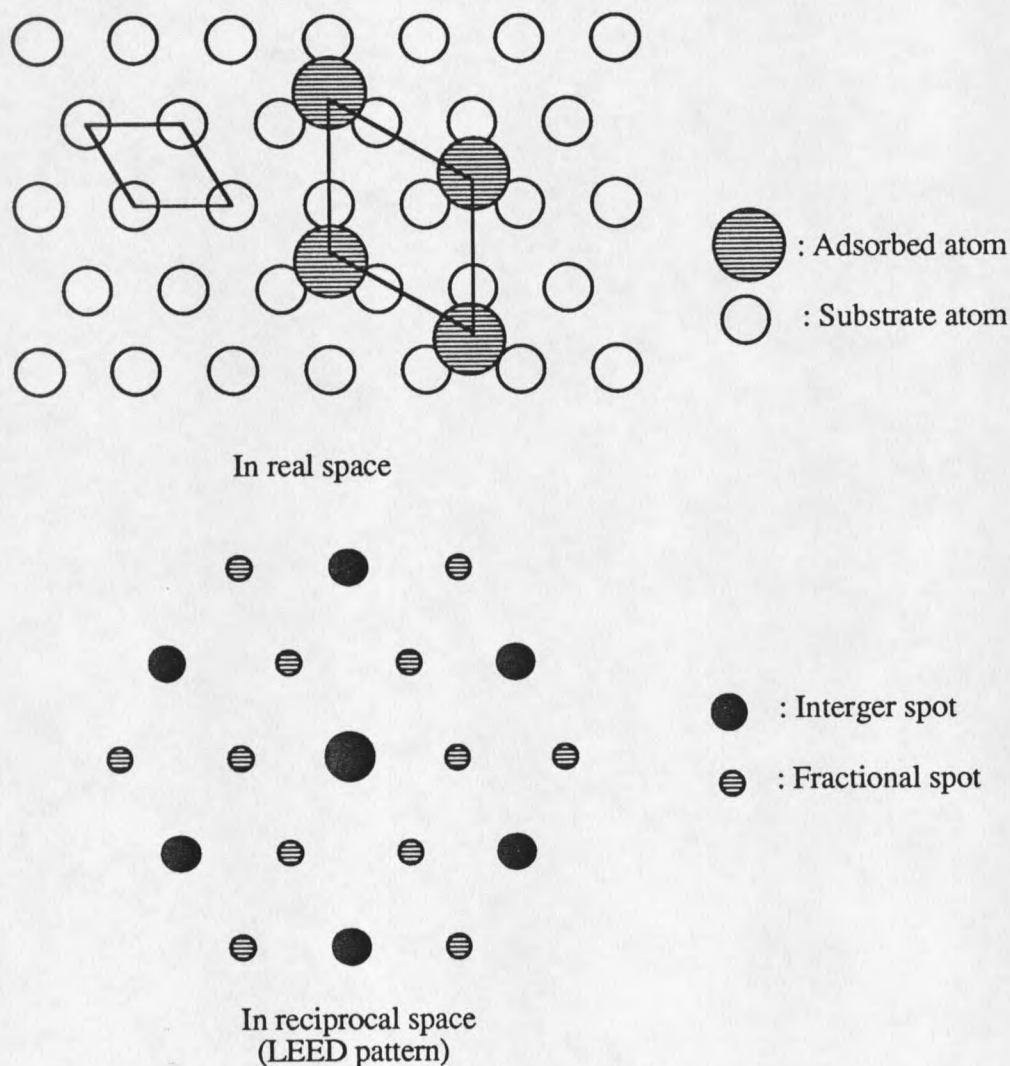


Fig. 2: The $(\sqrt{3}\times\sqrt{3})$ structure in reciprocal space and possible atomic arrangement in real space.

For every two-dimensional lattice, there exists a corresponding reciprocal lattice whose primitive vectors, $(\mathbf{a}_1^*, \mathbf{a}_2^*)$ satisfy

$$\mathbf{a}_i \cdot \mathbf{a}_j^* = 2\pi \delta_{ij} \quad (2.2)$$

Therefore, the $(\mathbf{a}_1^*, \mathbf{a}_2^*)$ can be determined from the equation:

$$\mathbf{a}_j^* = \frac{2\pi}{a_i \sin\gamma} \quad \text{and}$$

$$\mathbf{a}_i^* \perp \mathbf{a}_j \quad \text{for } i \neq j$$

Here γ is the angle between \mathbf{a}_1 and \mathbf{a}_2 . The utility of reciprocal space analyses in LEED is that the diffraction pattern is a direct representation of the reciprocal lattice, as shown next.

Low Energy Electron Diffraction (LEED)

Having established the classification of periodic surface structures, we can elucidate the physical origin of electron diffraction phenomena. The discovery of interference phenomena in processes where electrons are scattered by crystals played an important role in the development of quantum mechanics. L. de Broglie²⁸ postulated that an electron (or any particle) with velocity v and mass m exhibits a wave nature with wavelength $\lambda = h/mv$, h being Planck's constant. Thus, the wavelength for 100 eV-electrons is about 1.2 Å, a value which leads to interference in periodic crystal lattices. The technique of LEED uses an electron gun to generate a collimated beam of electrons which is then aimed at a crystal surface. The electrons scatter off the surface according to processes that depend on the geometry of the surface, as well as its elemental composition.

The surface sensitivity of LEED results from two effects. First, in the LEED energy range the mean-free-path for inelastic scattering of the electron is very short,

typically only about 5 Å. The properties of this parameter are discussed more extensively in the following chapter, but we note that LEED operates in the energy range in which the mean-free-path is typically at its smallest value, so that electrons penetrating more than two or three atomic layers into the solid have a high probability of losing energy (and coherence) relative to the incident beam and thus being lost from the elastically diffracted flux. A second source of surface sensitivity in LEED is the elastic scattering itself; backscattering is very strong (ion core cross-sections may be as large as 1 Å²) so that successive atom layers receive smaller incident electron fluxes and contribute less to the scattering. Typically, these two effects contribute equally to the surface sensitivity.

The formation of a diffraction pattern is illustrated schematically in Fig. 3. Here \mathbf{a}_1 and \mathbf{a}_2 are the unit vectors in real space. The wave vector \mathbf{k}_0 characterizes the incident wave, and the directions of interference maxima are determined by a set of wave vectors \mathbf{k} . \mathbf{k}_0 and \mathbf{k} must satisfy the well-known Bragg law:

$$\mathbf{k} - \mathbf{k}_0 = \mathbf{q} = h \mathbf{a}_1^* + k \mathbf{a}_2^* \quad (2.3)$$

where \mathbf{q} is any reciprocal lattice vector, \mathbf{a}_1^* and \mathbf{a}_2^* are the reciprocal unit vectors, and h and k are integers. The Bragg law is equivalent to the Laue condition,²⁹ which determines the allowed diffraction events consistent with translational invariance in two dimensions. This can be seen by multiplying Equation (2.3) by \mathbf{a}_1 and \mathbf{a}_2 :

$$\mathbf{a}_1 \cdot (\mathbf{k} - \mathbf{k}_0) = h \mathbf{a}_1 \cdot \mathbf{a}_1^* + k \mathbf{a}_1 \cdot \mathbf{a}_2^* = h$$

$$\mathbf{a}_2 \cdot (\mathbf{k} - \mathbf{k}_0) = h \mathbf{a}_2 \cdot \mathbf{a}_1^* + k \mathbf{a}_2 \cdot \mathbf{a}_2^* = k \quad (2.4)$$

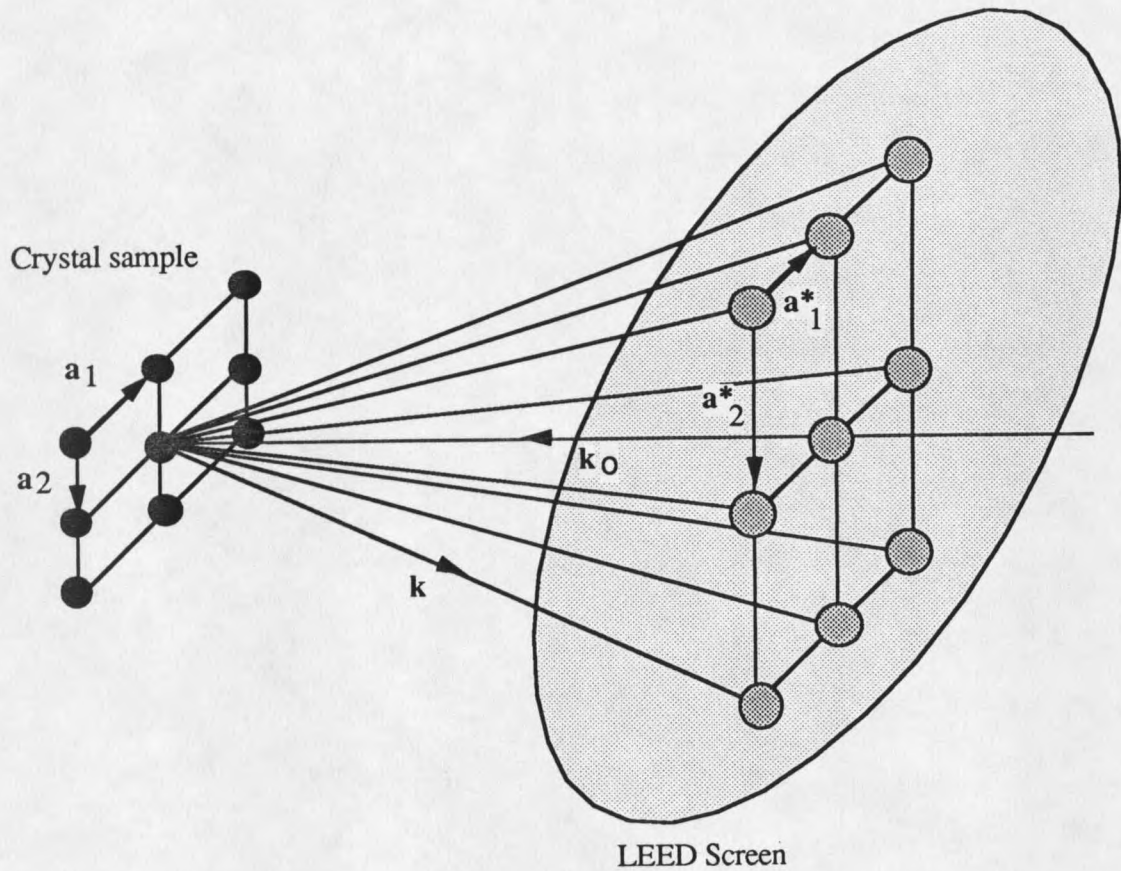


Fig. 3: The principle of the formation of a diffraction pattern in LEED experiment.

The vectors \mathbf{k} specify the directions of interference maxima; these are given by the points where the diffracted beams intersect the fluorescent screen, displaying the "diffraction spots" in LEED experiments. From the Equations (2.3) and (2.4), one can see that the LEED pattern is an image of the surface reciprocal lattice when viewed along the surface normal at a great distance from the crystal. To determine the directions of the scattered beams, one uses the Ewald construction. Since for a purely planar lattice mesh the periodic repeat distance is effectively infinite in the z direction, the reciprocal lattice "points" along the surface normal are infinitely dense - one speaks of a rod in reciprocal space. The Ewald sphere is constructed with a radius of $2\pi/\lambda$ and is centered at a point

